Journal of Quantitative Spectroscopy & Radiative Transfer 112 (2011) 2630–2637

Contents lists available at ScienceDirect

Journal of Quantitative Spectroscopy & Radiative Transfer

journal homepage: www.elsevier.com/locate/jqsrt

Notes

A linearized two-stream radiative transfer code for fast approximation of multiple-scatter fields

R. Spurr [a,*], V. Natraj [b]

[a] RT Solutions, Inc. 9 Channing Street, Cambridge, MA 02138, USA
[b] Jet Propulsion Laboratory, California Institute of Technology, 4800 Oak Grove Drive, Pasadena, CA 91109, USA

ARTICLE INFO

Article history:
Received 19 May 2011
Received in revised form
21 June 2011
Accepted 23 June 2011
Available online 23 July 2011

Keywords:
2-Stream
Radiative transfer
Jacobians
Multiple-scatter accuracy

ABSTRACT

Performance is an issue for radiative transfer simulations in hyper-spectral remote sensing backscatter retrieval algorithms. 2-Stream models are often used to speed up flux and radiance calculations. Here we present a linearized 2-stream multiple-scatter code, with the ability to generate analytic weighting functions with respect to any atmospheric or surface property. We examine 2-stream accuracy for the satellite intensity diffuse field, and the corresponding Jacobians for total ozone column and surface albedo, for an application in the ozone UV Huggins bands.

1. Introduction

The 2-stream (2S) approximation for anisotropic scattering in an optically homogeneous medium offers an insightful and analytically straightforward approach to understanding a wide variety of radiative transfer (RT) problems. The 2S method goes back more than 100 years to the work of Schuster and Schwarzschild in 1905, and the well-known Eddington approximation for 2S RT was introduced in 1916 (see [1] for historical references).

There are a number of 2S codes written for inhomogeneous multi-layer atmospheres; examples may be found in [2–4]. Although the RT equation may be written down as in Eq. (1) below for each layer n in a stratification of optically uniform layers, it is necessary to determine the solution of the boundary value problem using linear matrix algebra. 2S codes have been embedded in a number of global transport models for the fast calculation of fluxes and heating rates essential to studies of radiative forcing and climate modeling.

Accuracy for 2S approximations was explored by a number of authors such as [5], and as noted by [1], the use of the delta-M 2S scaling approximation (for treating sharply peaked phase functions) is particularly important for the accuracy of the 2S method. Multi-layer 2S results have been compared for accuracy against the well-known DISORT model [6]. 2S RT models are not accurate enough for remote sensing retrievals using UV/Visible backscatter measurements, even when an accurate calculation is made for the single-scatter radiation field and the 2S calculation is confined to the multiple-scatter diffuse-field contributions.

However, recent developments in increasing performance speed for hyper-spectral applications have led to renewed interest in 2S models. For example, retrievals of the column-averaged dry air mole fraction of CO_2 (X_{CO_2}) from measurements taken by the Orbiting Carbon Observatory instrument [7] require many thousands of RT simulations of backscattered light in three near-infrared windows (O_2 A band around 0.76 μm, weak and strong CO_2 absorption bands centered at 1.61 and 2.06 μm, respectively). In this regard, Principal Component Analysis

* Corresponding author. Tel.: +1 617 492 1183.
E-mail address: rtsolutions@verizon.net (R. Spurr).

0022-4073/$ - see front matter © 2011 Elsevier Ltd. All rights reserved.
doi:10.1016/j.jqsrt.2011.06.014

(PCA) was performed on the differences [8] or logarithm of ratios [9] between 2S and DISORT reflectances for the *P* and *R* branches of the *A* band to obtain an order of magnitude improvement in speed. More recently, [10] presented a Low-stream Interpolator (LSI) method for speeding-up hyper-spectral calculations of multiple-scatter reflectance fields; this is based in part on the optical property analysis method of [11] applied to 2S residuals.

In recent years, a number of atmospheric radiative transfer models have been developed with the "linearization" capability; that is, the generation of analytic weighting functions (Jacobians), which are the partial derivatives of the radiation field with respect to atmospheric and surface parameters [12–14]. Jacobians are particularly important for retrieval applications involving nonlinear least squares fitting (with and without regularization); a classic example is the derivation of ozone profiles from UV backscatter instruments such as GOME and OMI [15]. Jacobians may be defined with respect to any profile of atmospheric constituents, or to any parameter pertinent to the whole atmosphere (such as a trace gas total column), or to any surface property such as the albedo. The discrete ordinate LIDORT RT model (see [16] for a recent review) has all these linearization capabilities.

In this paper, we focus on a fully-linearized 2S model for the multiple-scatter radiation fields in a multi-layer atmosphere. Output is confined to the most common applications (upwelling top of atmosphere, downwelling surface field). We include the pseudo-spherical treatment of solar beam attenuation in a curved atmosphere and the implementation of the delta-M 2S approximation. Output from the 2S model is validated against LIDORT results (running with 2 discrete ordinates).

Section 2 provides a short summary of the 2S theory. The linearization is treated in more detail in Section 3. The example in Section 4 examines accuracy for radiances and 2 types of Jacobians in the retrieval of total ozone amounts from UV backscatter measurements.

2. Summary of 2S theory

In the 2S approximation, the azimuthal expansion of the radiation field is restricted to the first two terms: $I(\mu,\varphi)=I_0(\mu)+2I_1(\mu)\cos\varphi$. The phase function $\Phi(\Theta)$ is assumed to have a Legendre polynomial expansion $\Phi(\Theta)=\Sigma_{l=0}^{2}\beta_l P_l(\cos\Theta)$ in terms of the cosine of the scattering angle Θ. We require the first two terms with expansion coefficients $\beta_0=1$ and $\beta_1=3g$, where g is the asymmetry parameter, to solve the 2S equations, while the third term involving β_2 is needed for the delta-M 2S scaling approximation (see below). For single-scatter albedo ω and optical depth coordinate x, the 2S plane-parallel radiative transfer equations in a single optically homogeneous layer are

$$\overline{\mu}\frac{dI^{\pm}}{dx}=I^{\pm}\left[1-\omega(1-b)\right]-\omega bI^{\mp}-\frac{\omega F_{*}}{4\pi}b^{\pm}(\mu_0)Te^{-\eta x}. \qquad (1)$$

Here $\overline{\mu}$ is the stream direction for the upwelling and downwelling fields I^- and I^+ respectively, μ_0 is the cosine of the solar angle, and F_* is the solar flux. For the standard choice $\overline{\mu}=\sqrt{1/3}$, the backscatter coefficients are $b=(1/2)(1-g)$ and $b^{\pm}(\mu_0)=(1/2)(1\mp 3g\overline{\mu}\mu_0)$. Solar beam attenuation is written as $Te^{-\eta x}$ in the pseudo-spherical approximation, where T is the beam transmittance to the top of the layer, and $e^{-\eta x}$ is the in-layer transmittance expressed in terms of an "average secant" η [17]. For plane-parallel attenuation, $\eta=1/\mu_0$.

These equations are easily solved by means of exponential substitutions $\sim X^{\pm}e^{-kx}$ for the homogeneous solutions, and $\sim W^{\pm}e^{(-\eta x)}$ for the particular integral. Thus, the solution for any Fourier component $I^{\pm}(\overline{\mu},x)$ can be written

$$I^{\pm}(\overline{\mu},x)=AX^{\pm}(\overline{\mu})e^{-kx}+BX^{\mp}(\overline{\mu})e^{-k(\Delta-x)}+W^{\pm}(\overline{\mu})e^{-\eta x}. \qquad (2)$$

In this equation, A and B are integration constants for the homogeneous solutions; these are determined by boundary conditions. Here, Δ is the layer total optical thickness, and the presence of the exponential $e^{-k(\Delta-x)}$ in the second term ensures that solutions remain bounded.

The choice of stream direction $\overline{\mu}$ depends on the quadrature scheme. For a full quadrature over both hemispheres $[-1, 1]$, values of $\overline{\mu}$ are the zeros of the second Legendre polynomial $P_2(\mu)$, i.e. $\overline{\mu}=\pm 1/\sqrt{3}$. For double-Gauss quadrature over the two hemispheric intervals $[-1, 0]$ and $[0, 1]$, we have $\overline{\mu}=\pm 0.5$. Both quadrature options have been implemented in this work. Table 1 contains details of the solutions in Eq. (2); the quantity c is defined by $c=3\omega g$. These results may be found in the

Table 1
2-Stream solutions (quadrature and post-processed).

Solution type	Fourier component $m=0$	Fourier component $m=1$
1. 2S homogeneous solution: $k=\sqrt{sd}$; $X^{\pm}=\frac{1}{2}\left[1\mp\frac{s}{k}\right]$	$d=\frac{1}{\overline{\mu}}\left[c\overline{\mu}^2-1\right]$, $s=\frac{1}{\overline{\mu}}(\omega-1)$	$d=-\frac{1}{\overline{\mu}^2}$, $s=\frac{[c(1-\overline{\mu}^2)-2]}{2\overline{\mu}}$
2. 2S particular integral $W^{\pm}=\frac{1}{2}T[Z\pm Y]$; $Z=\frac{\eta Q^- -dQ^+}{k^2-\eta^2}$; $Y=\frac{sZ-Q^+}{\eta}$	$Q^+=\frac{F_*}{2\pi}\frac{\omega}{\overline{\mu}}Q^-=\frac{F_*}{2\pi}c\mu_0$	$Q^+=\frac{cF_*}{4\pi\overline{\mu}}\sqrt{(1-\overline{\mu}^2)(1-\mu_0^2)}$ $Q^-=0$
3. Post-processed homogeneous solutions $U(\mu)$ in polar direction μ	$U^{\pm}(\mu)=\frac{1}{2}X^-(\omega+c\mu\overline{\mu})\pm\frac{1}{2}X^+(\omega-c\mu\overline{\mu})$	$U^{\pm}(\mu)=\pm\frac{c\overline{\mu}}{2}(X^- -X^+)\sqrt{\frac{1}{2}(1-\mu^2)}$
4. Post-processed diffuse-field particular integrals $G(\mu)$ in polar direction μ	$G^{\pm}(\mu)=\frac{1}{2}W^-(\omega\pm c\mu\overline{\mu})+\frac{1}{2}W^+(\omega\mp c\mu\overline{\mu})$	$G^{\pm}(\mu)=\frac{c}{4}(W^- -W^+)\sqrt{\frac{1}{2}(1-\mu^2)(1-\overline{\mu}^2)}$
5. Post-processed single-scatter particular integrals $\Gamma(\mu)$ in polar direction μ	$\Gamma^{\pm}(\mu)=-\frac{F_*}{4\pi}(\omega\pm c\mu\mu_0)$	$\Gamma^{\pm}(\mu)=\frac{F_* c}{8\pi}\sqrt{(1-\mu^2)(1-\mu_0^2)}$
6. Post-processed homogeneous solution multipliers $H(\mu)$	$H^+(\mu)=\frac{e^{-k\Delta}-e^{-\Delta/\mu}}{1-k\mu}$; $H^-(\mu)=\frac{1-e^{-k\Delta}e^{-\Delta/\mu}}{1+k\mu}$	
7. Post-processed particular integral multipliers $E(\mu)$	$E^+(\mu)=T\frac{e^{-\eta\Delta}-e^{-\Delta/\mu}}{1-\eta\mu}$; $E^-(\mu)=T\frac{1-e^{-\eta\Delta}e^{-\Delta/\mu}}{1+\eta\mu}$	

literature; for example, [1] has a thorough review of the 2S approximation, including a discussion on the choice of quadrature.

In a stratified N-layer atmosphere with layer optical depths $\{\Delta_n\}$, the boundary conditions are

(1) Downwelling diffuse field at the upper boundary is zero: $I_n^+(\overline{\mu},0)=0$ for $n=1$;
(2) Continuity at intermediate layer boundaries ($n=2$, …, N): $I_{n-1}^{\pm}(\overline{\mu},\Delta_{n-1})=I_n^{\pm}(\overline{\mu},0)$;
(3) Surface reflection (assumed Lambertian), for layer N: $I_N^-(\overline{\mu},\Delta_N)=\overline{\mu}RI_N^+(\overline{\mu},\Delta_N)$.

Application of these conditions results in a sparse linear algebra system $\mathbf{MX}=\mathbf{B}$ where $\mathbf{X}$ is the vector of unknown integration constants, $\mathbf{M}$ is a matrix constructed from homogeneous solutions, and $\mathbf{B}$ is a column vector constructed from particular integrals. The system has the form

$$\begin{pmatrix} X_1^+ & X_1^-\Omega_1 & 0 & 0 & 0 & 0 & 0 & \dots & 0 & 0 \\ X_1^+\Omega_1 & X_1^- & -X_2^+ & -X_2^-\Omega_2 & 0 & 0 & 0 & \dots & 0 & 0 \\ X_1^-\Omega_1 & X_1^+ & -X_2^- & -X_2^+\Omega_2 & 0 & 0 & 0 & \dots & 0 & 0 \\ 0 & 0 & X_2^+\Omega_2 & X_2^- & -X_3^+ & -X_3^-\Omega_3 & 0 & \dots & 0 & 0 \\ 0 & 0 & X_2^-\Omega_2 & X_2^+ & -X_3^- & -X_3^+\Omega_3 & 0 & \dots & 0 & 0 \\ 0 & 0 & 0 & 0 & X_3^+\Omega_3 & X_3^- & -X_4^+ & \dots & 0 & 0 \\ 0 & 0 & 0 & 0 & X_3^-\Omega_3 & X_3^+ & -X_4^- & \dots & 0 & 0 \\ \dots & \dots & \dots & \dots & \dots & \dots & \dots & \dots & \dots & \dots \\ \dots & \dots & \dots & \dots & \dots & \dots & \dots & \dots & \dots & \dots \\ 0 & 0 & 0 & 0 & 0 & 0 & 0 & \dots & V_N^-\Omega_N & V_N^+ \end{pmatrix} \otimes \begin{pmatrix} A_1 \\ B_1 \\ A_2 \\ B_2 \\ A_3 \\ B_3 \\ A_4 \\ \dots \\ A_N \\ B_N \end{pmatrix} = \begin{pmatrix} -W_1^+ \\ W_2^+ - W_1^+\Lambda_1 \\ W_2^- - W_1^-\Lambda_1 \\ W_3^+ - W_2^+\Lambda_2 \\ W_3^- - W_2^-\Lambda_2 \\ W_4^+ - W_3^+\Lambda_3 \\ W_4^- - W_3^-\Lambda_3 \\ \dots \\ \dots \\ -K_N^-\Lambda_N \end{pmatrix}. \quad (3)$$

Here we have defined $V_N^{\pm}=X_N^{\pm}-\overline{\mu}RX_N^{\mp}$, $K_N^-=W_N^--\overline{\mu}RW_N^+$, $\Omega_n=e^{-k_n\Delta_n}$, $\Lambda_n=e^{-n_n\Delta_n}$. It is of course possible to solve this system using a standard package such as the LAPACK software (this is the LIDORT default). However, matrix $\mathbf{M}$ has pentadiagonal form, and we adapted a "pentadiagonal solver" from the Internet (http://cococubed.asu.edu/codes/penta/matrix_pent.f); this turned out to be considerably faster than the LAPACK solution. Once found, the inverse $\mathbf{M}^{-1}$ is stored and then applied repeatedly in the back substitutions required for solution of the linearized boundary value problem (next section).

For the radiation field at polar cosines μ away from quadrature $\overline{\mu}$, we use the source function integration technique, following the LIDORT methodology. For the 2S upwelling field at top of atmosphere (TOA) in polar direction μ, we may write

$$I_0^-(\mu)=I_N^-(\mu)e^{-\tau_N/\mu}+\sum_{n=1}^{N}S_n^-(\mu)e^{-\tau_n/\mu}. \quad (4)$$

$$S_n^-(\mu)=A_nU_n^-(\mu)H_n^-(\mu)+B_nU_n^+(\mu)H_n^+(\mu)+E_n^-(\mu)[G_n^-(\mu)+\Gamma_n^-(\mu)]. \quad (5)$$

Here $I_N^-(\mu)$ is the surface upwelling field (bottom of layer N), $\tau_n=\Sigma_{k=1}^{n-1}\Delta_k$ is the cumulative vertical optical depth to layer n ($\tau_1=0$), and $S_n^-(\mu)$ the upwelling source term for layer n. The latter is expressed in terms of the integration constants A_n and B_n for that layer, the solutions $U_n^{\pm}(\mu)$, $G_n^-(\mu)$ and $\Gamma_n^-(\mu)$, and the multipliers $H_n^{\pm}(\mu)$ and $E_n^-(\mu)$. Expressions for these solutions and multipliers are written down in Table 1, rows 3–7. Similar expressions can be derived for the downwelling fields.

Multiple-scatter solutions. As noted earlier, we have constructed our model to operate in "multiple-scatter" (MS) mode. This means that contributions involving the post-processed single-scatter term $\Gamma(\mu)$ (row 5 in Table 1) are omitted from the calculation. Indeed, the 2S single-scatter (SS) contributions are based on severely truncated phase function information, and in practical applications it makes sense to replace these terms by accurate single-scatter RT calculations using the full phase function. Thus our model computes the modified source terms

$$\tilde{S}_n^-(\mu)=A_nU_n^-(\mu)H_n^-(\mu)+B_nU_n^+(\mu)H_n^+(\mu)+E_n^-(\mu)G_n^-(\mu). \quad (6)$$

In applications, we look at the combination "Exact SS+2S MS" to estimate the full radiation field. We will use the LIDORT code as our benchmark, both to provide the accurate single-scatter result and the multiple-stream MS result.

Delta-M approximation. The delta-M scaling partially compensates for loss of information associated with phase function truncation in the use of quadrature sums to approximate multiple-scatter integrals. The phase function is written $\Phi(\Theta)=f\delta(1-\cos\Theta)+(1-f)\overline{\Phi}(\Theta)$, in terms of a delta-function in the forward direction and a smoother counterpart $\overline{\Phi}(\Theta)$, where f is the delta-M scaling factor. Substitution of this scaled phase function yields another RT equation of the same form, but with scaled optical properties given by

$$\overline{\Delta}=\Delta(1-\omega f);\quad \overline{\omega}=\frac{\omega(1-f)}{(1-\omega f)};\quad \overline{g}=\frac{g-f}{1-f}. \quad (7)$$

In the 2S approximation, one choice of f is to set it equal to g. In this case, the delta-M scaled RT equation becomes isotropic. For anisotropic scattering applications in 2S, we use the β_2 phase function expansion coefficient and set $5f=\beta_2$. For the Henyey–Greenstein phase function, we have $\beta_2=5g^2$, from which we obtain $\overline{g}=g/(1+g)$. This special case illustrates the importance of the 2S

scaling, since $\overline{g} < 0.5$, and the resulting scaled 2S equations are much more accurate for reduced values of g.

3. 2S weighting functions

In order to obtain Jacobians of the radiation field, we differentiate analytically the complete 2S solution with respect to any profile, column, or surface variable. For an *atmospheric* variable ξ, the Jacobian will depend on derivatives of the input optical properties (IOPs) with respect to ξ. Writing $\mathcal{L}(y) \equiv \partial y/\partial\xi$ for the linearization operator, we define IOP derivatives $\mathcal{L}(\Delta)$, $\mathcal{L}(\omega)$ and $\mathcal{L}(c) = 3[\omega\mathcal{L}(g) + g\mathcal{L}(\omega)]$. Since all solutions in Table 1 are linearly dependent on the IOPs, differentiation is achieved by repeated application of the chain rule. For eigensolutions (row 1)

$$\mathcal{L}(X^{\pm}) = \pm\frac{s\mathcal{L}(k) - k\mathcal{L}(s)}{2k^2}; \quad \mathcal{L}(k) = \frac{1}{2}\sqrt{\frac{d\mathcal{L}(s)}{s} + \frac{s\mathcal{L}(d)}{d}}. \tag{8}$$

Here $\mathcal{L}(d) = \overline{\mu}\mathcal{L}(c)$ and $\mathcal{L}(s) = \mathcal{L}(\omega)/\overline{\mu}$ for Fourier component $m=0$, with $\mathcal{L}(d) = 0$, and $\mathcal{L}(s) = \frac{1}{2}\mathcal{L}(c)(1-\overline{\mu}^2)/\overline{\mu}$ for Fourier component $m=1$. In a similar vein, derivatives of the post-processed homogeneous solution (rows 3 and 6 in Table 1) may be established in terms of $\mathcal{L}(\Delta)$, $\mathcal{L}(\omega)$, and $\mathcal{L}(c)$. In a multi-layer atmosphere, homogeneous solutions in layer n depend only on IOPs in this layer, so that Eq. (8) is valid for all layers— there are no cross-layer derivatives.

However, for the particular integral in layer n, there is some dependency on IOPs in layers above and including n. This is because of the solar beam attenuation through layers $p \le n$. We differentiate the layer n solutions with respect to parameters in layer p to find

$$\mathcal{L}_p(W_n^{\pm}) = \frac{1}{2}\left[\mathcal{L}_p(T_n)(Z_n \pm Y_n) + T_n\left\{\mathcal{L}_p(Z_n) \pm \mathcal{L}_p(Y_n)\right\}\right]. \tag{9}$$

$$\mathcal{L}_p(Z_n) = \frac{Q_n^- \mathcal{L}_p(\eta_n) + \eta_n\delta_{np}\mathcal{L}_n(Q_n^-) - \delta_{np}[d_n\mathcal{L}_n(Q_n^+) + Q_n^+\mathcal{L}_n(d_n)]}{k_n^2 - \eta_n^2} - Z_n\frac{2\delta_{np}k_n\mathcal{L}_n(k_n) - 2\eta_n\mathcal{L}_p(\eta_n)}{k_n^2 - \eta_n^2}. \tag{10}$$

Here δ_{np} is the Kronecker delta. $\mathcal{L}_p(Y_n)$ follows from Eq. (10) and the definition in row 2 of Table 1. Derivatives $\mathcal{L}_n(Q_n^{\pm})$ are determined easily from the table entries. Cross-layer derivatives only arise through the solar beam initial-layer transmittances T_n and the average secants η_n. Differentiation of this pseudo-spherical parameterization follows LIDORT methodology [17]. For the plane-parallel case, $T_n = \exp[-\tau_n/\mu_0]$, so that $\mathcal{L}_p(T_n) = -\mathcal{L}_p(\Delta_p)T_n/\mu_0$ and $\mathcal{L}_p(\eta_n) = 0$ (where $\tau_n = \Sigma_{k=1}^{n-1}\Delta_k$). The rest of the particular integral contributions (rows 2, 4, 5, and 7 in Table 1) may now be differentiated, bearing in mind the existence of cross-layer derivatives.

Next, we differentiate the linear algebra system $\mathbf{MX} = \mathbf{B}$ in order to obtain the integration constant derivatives $\mathcal{L}_k(A_n)$ and $\mathcal{L}_k(B_n)$. We find

$$\mathbf{M}\mathcal{L}_k(\mathbf{X}) = \mathbf{B}'_k \equiv \mathcal{L}_k(\mathbf{B}) - \mathcal{L}_k(\mathbf{M})\mathbf{X}. \tag{11}$$

This is a related linear algebra system with the same matrix, but a new column vector. The solution $\mathcal{L}_k(\mathbf{X})$ is readily available by back substitution, since we have already the inverse matrix $\mathbf{M}^{-1}$ from the solution of the original boundary value problem. Construction of the new column vector depends on the derivative matrices $\mathcal{L}_k(\mathbf{M})$ and $\mathcal{L}_k(\mathbf{B})$. The former is constructed from homogeneous solution derivatives, the latter from particular integrals—an inspection of the entries in Eq. (3) reveals the nature of this straightforward piece of chain-rule differentiation. Jacobians for the post-processed solutions in Eqs. (4) and (6) may be determined also by repeated chain-rule differentiation of all the necessary entries in these equations.

We remark on the differences between *profile* and *column* linearization. For profile Jacobians, the above linearization procedure must be repeated for every layer, and for every variable in a given layer for which a Jacobian is desired. Now suppose we require a Jacobian with respect to a whole-atmosphere property σ (e.g. total column of trace species, or total aerosol optical depth). Optical properties in *every* layer will depend on σ, so that the set $\{\mathcal{L}_n(\Delta_n),\ \mathfrak{L}_n(\omega_n),\ \mathfrak{L}_n(c_n)\}$ of IOP derivatives will be the end points for the chain rule differentiation. The derivative procedure is the same as before, with the exception of solar beam attenuation. For example, from the definition of T_n, we have $\mathcal{L}_\sigma(T_n) = \exp[-\Sigma_{k=1}^{n-1}\mathcal{L}_\sigma(\Delta_k)/\mu_0]$ for the plane-parallel beam.

Lastly, we treat surface property Jacobians; for simplicity considering here just the Lambertian case. If $\mathcal{L}_R$ denotes linearization with respect to albedo R, then derivatives of all solution entries in Table 1 are absent (none depend on R). However, integration constant derivatives $\mathcal{L}_R(A_n)$ and $\mathcal{L}_R(B_n)$ will be determined from $\mathcal{L}_k(\mathbf{X}) = \mathbf{M}^{-1}[\mathcal{L}_R(\mathbf{B}) - \mathcal{L}_R(\mathbf{M})\mathbf{X}]$. From Eq. (3), only entries in the final rows of $\mathbf{M}$ and $\mathbf{B}$ depend on R; the corresponding derivative is easy to write down. Once the boundary problem is linearized, the post-processed solution can then be differentiated with respect to R in order to get the final Jacobian. The procedure for non-Lambertian BRDFs is similar, and has been implemented in the present model—for details in the general LIDORT case, see [16].

Finally, we note that the delta-M expressions in Eq. (7) may be differentiated easily from knowledge of $\mathcal{L}(\Delta)$, $\mathcal{L}(\omega)$ and $\mathcal{L}(g)$, and the derivative $\mathcal{L}(f)$; see the discussion in [17].

4. Multiple-scatter 2S accuracy: an example for UV ozone

The application considered here is for the retrieval of total ozone column amounts from moderate-resolution atmospheric chemistry instruments such as GOME-1 (launched 1995), SCIAMACHY (launched 2002), GOME-2 [18], and OMI [19]. This retrieval is traditionally performed using Differential Optical Absorption Spectroscopy (DOAS) methods involving absorber slant column fitting followed by Air Mass Factor (AMF) RT simulations to make the conversions to vertical column amounts. A typical fitting window is 325–335 nm in the ozone Huggins bands absorption regime; scattering is Rayleigh dominated and AMF calculations (at one wavelength) must be performed using a full MS RT model. The operational GOME-1 DOAS algorithm for total ozone is described in [20].

Recently, a new algorithm has been developed for the direct fitting of total ozone in this UV window. The forward model will simulate all backscatter measurements together with 2 column Jacobians with respect to the total ozone amount and to the surface albedo; the inverse model is a loosely constrained least-squares fitting. This algorithm is more physically realistic than the DOAS approach; the latter really assumes that O_3 absorption is optically thin in the Huggins window—an approximation that is not always justified in reality. Initial direct fitting results for GOME-1 show improvements in several aspects over the DOAS values [21].

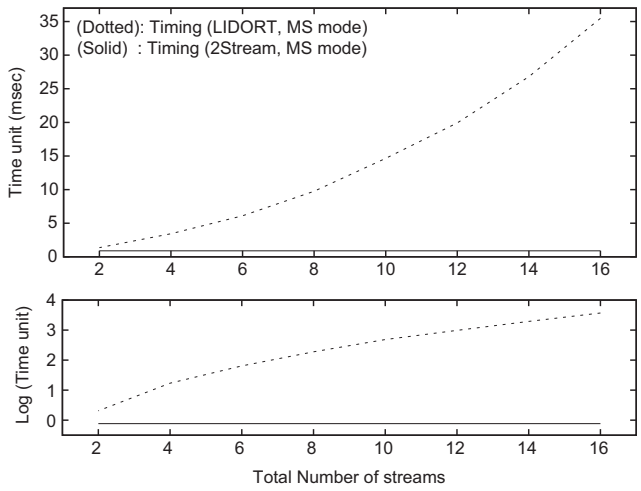

Fig. 1. Timing tests for 2S (solid line) against LIDORT (dotted line).

The direct fitting approach requires RT calculations for all wavelengths, and is an order of magnitude slower than its DOAS counterpart. Given the need for full MS computations, it is clearly of interest to examine the potential for 2S usage in this application.

In this regard, we examine 2S accuracy for a scenario comprising a 34-layer atmosphere with ozone trace gas absorption, Rayleigh scattering and aerosol content confined to a single cloud layer. The surface is assumed Lambertian. Ozone profiles for the RT simulations are taken from the TOMS Version 8 climatology [22]; this data is classified according to month, latitude zone and total ozone amount Ω. This climatology defines a unique correspondence between profile and total column. For gas absorption optical depth a_n in layer n, Rayleigh scattering optical depth σ_n, aerosol scattering depth for extinction τ_n, aerosol single scattering albedo z_n, and aerosol asymmetry parameter Γ_n, the 2S IOPs are

$$\Delta_n = a_n + \sigma_n + \tau_n; \quad \omega_n = \frac{\sigma_n + z_n\tau_n}{\Delta_n}; \quad c_n = \frac{3z_n\tau_n\Gamma_n}{\Delta_n}. \qquad (12)$$

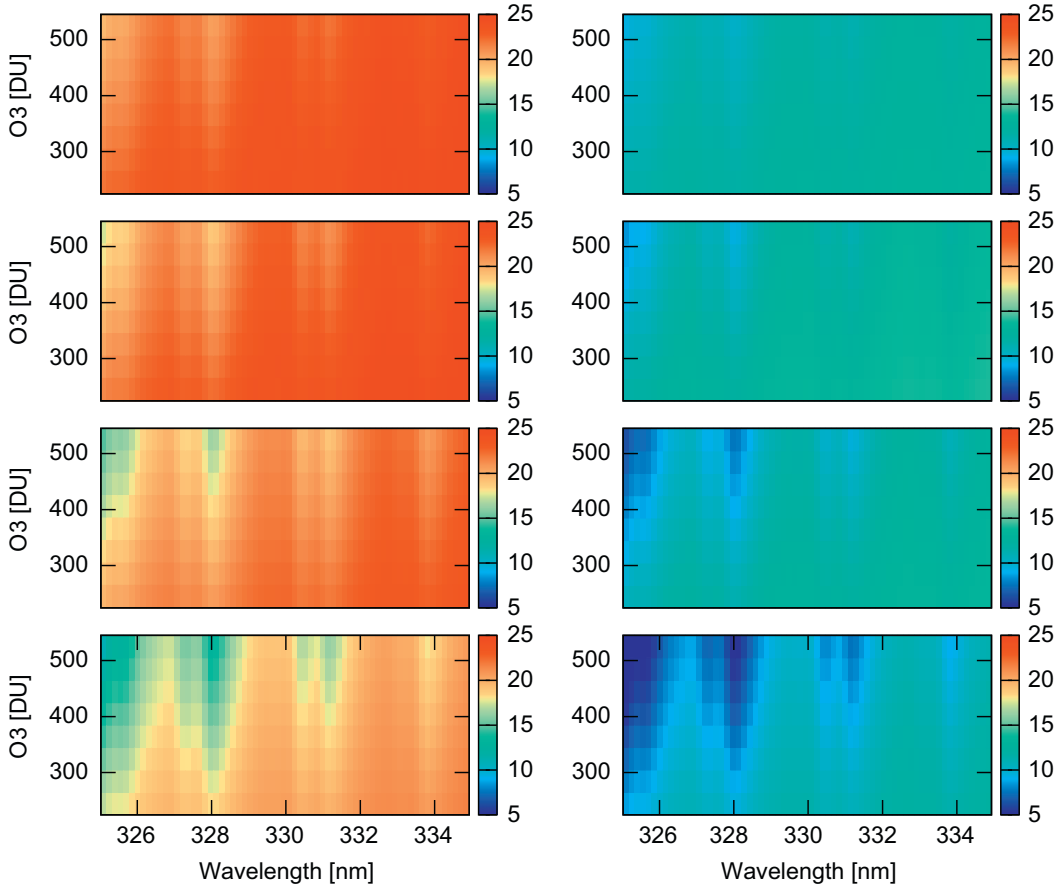

Fig. 2. Contour plots of relative MS intensity differences (in %) between 2S and L8, for wavelengths between 325 and 335 nm, and total ozone from 225 to 545 [DU]. (Left panels) Clear-sky scenario; (right panels) the same atmosphere with additional cloud of optical thickness 3.0 at 3–4 km. From top to bottom, plots are for the solar angles [45°, 60°, 70°, 77°].

Linearized IOPS depend on the profile derivative $\mathcal{L}_\Omega(a_n)$, which may be established most simply by assuming a linear correspondence between entries in the column-classified profile data set.

For the 325–335 nm range, we use a solar spectrum from the OMI instrument to provide a set of wavelengths for calculation (67 points). Rayleigh depolarization ratios and cross-sections are taken from [23], and ozone cross-sections from a pre-convolution applied to the Daumont–Malicet data [24]. We choose a temperature and pressure profile for a typical mid-latitude summer atmosphere. Runs were performed for some 9 total ozone amounts from 225 DU to 545 DU, for one viewing geometry (zenith 20°, azimuth 10°) and 7 solar zenith angles (25°, 45°, 60°, 70°, 77°, 82° and 85°). The single cloud layer was given optical thickness 3.0 between heights 3–4 km, with scattering properties determined by asymmetry parameter 0.8. Runs were made for clear-sky and cloud-filled cases, for all wavelengths, solar angles, and ozone columns.

First, we look at a few timing statistics for these runs, comparing 2S and LIDORT (both operating in MS-mode), with the number of LIDORT discrete ordinates running from 2 to 16 (full range). The 8-stream LIDORT (L8) calculation is the current default in the direct fitting work; Fig. 1 shows that our dedicated 2S model is an order of magnitude faster for this case. Note also the timing offset between our 2S model and LIDORT with 2 discrete ordinates—our model is 50% faster (this shows up better on the logarithmic plot).

Next we look at MS accuracy for the three simulated quantities central to this retrieval, namely, the total intensity and the total ozone and surface albedo Jacobians. In each case we show contour plots of the relative differences between our 2S model output and LIDORT 8-stream output (L8), against wavelength and total ozone amount. Fig. 2 has the intensity results; the left panels are clear-sky (Rayleigh-only) comparisons, the right panels show differences for the cloud-filled scenario. Results for 4 solar zenith angles are shown (45°, 60°, 70° and 77°, top to bottom). Figs. 3 and 4 show the two Jacobian results.

Finally we compare the full intensities including the accurate single-scatter computation. The SS result is computed separately in LIDORT, and this may be used in conjunction with the 2S result, so that the contours in Fig. 5 show relative differences between SS+2S and SS+L8 (2S and L8 are MS only calculations). These differences are smaller than those in Fig. 2, since the single-scatter contribution is the largest part of the radiance field for this wavelength window.

5. Concluding remarks

The linearized 2S software package described in this paper has been created in Fortran 77 and Fortran 90. The code is called as a simple subroutine with input and output lists; there are no dependencies (no data files, no common-block storage, no 'include', or 'module' statements). The software comes with a User Guide, which explains the

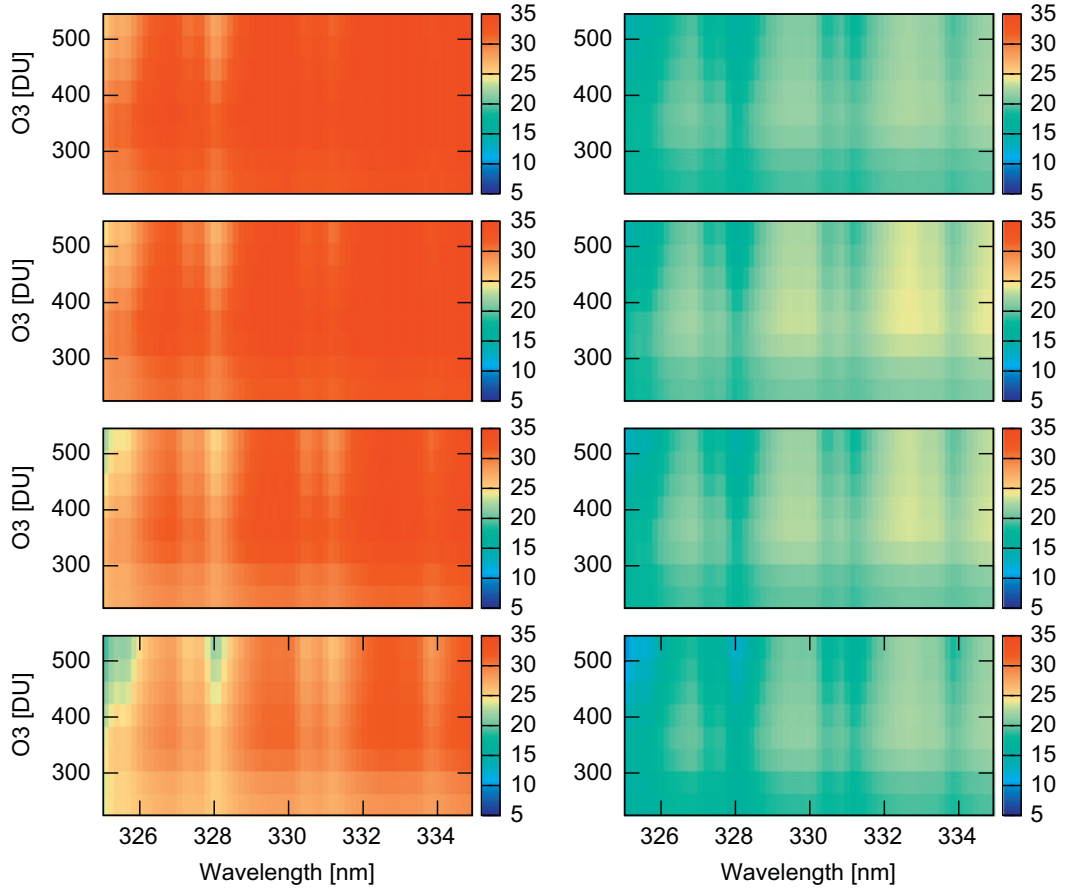

Fig. 3. Contour plots of relative MS total ozone Jacobian differences (in %) between 2S and L8. Scenarios as in Fig. 2.

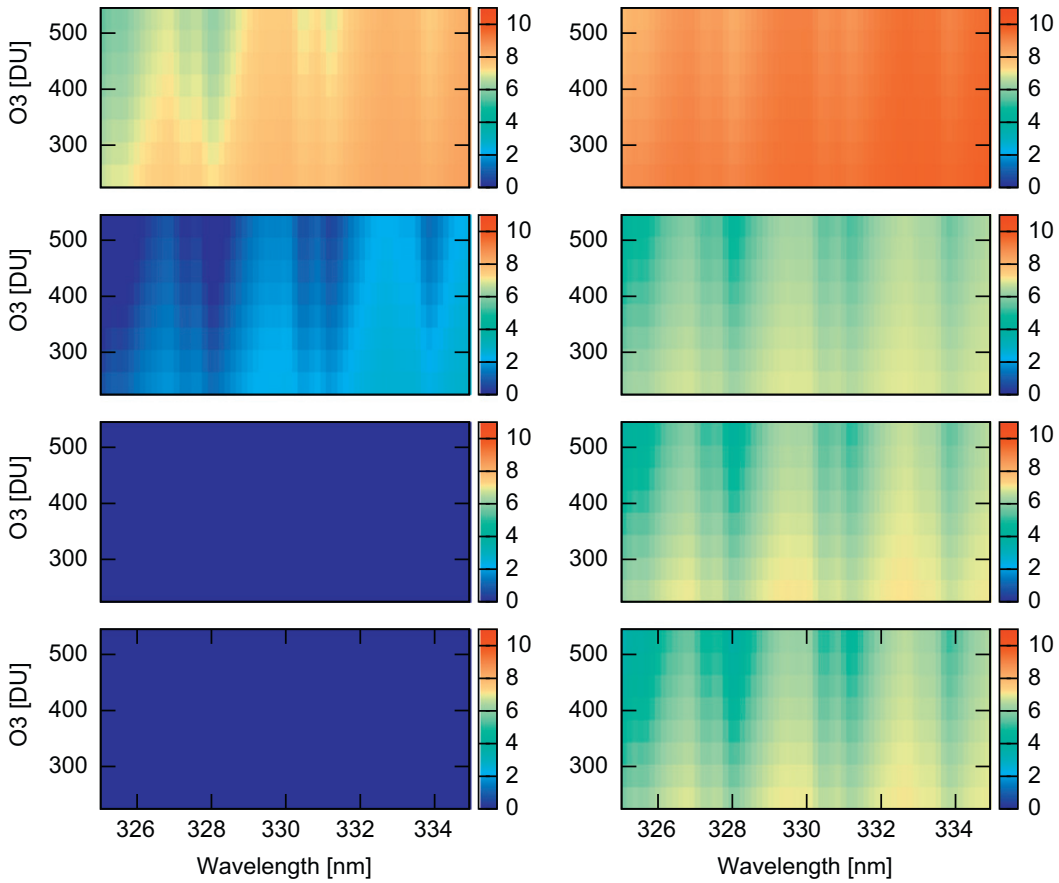

Fig. 4. Contour plots of relative MS Surface albedo Jacobian differences (in %) between 2S and L8. Scenarios as in Fig. 2.

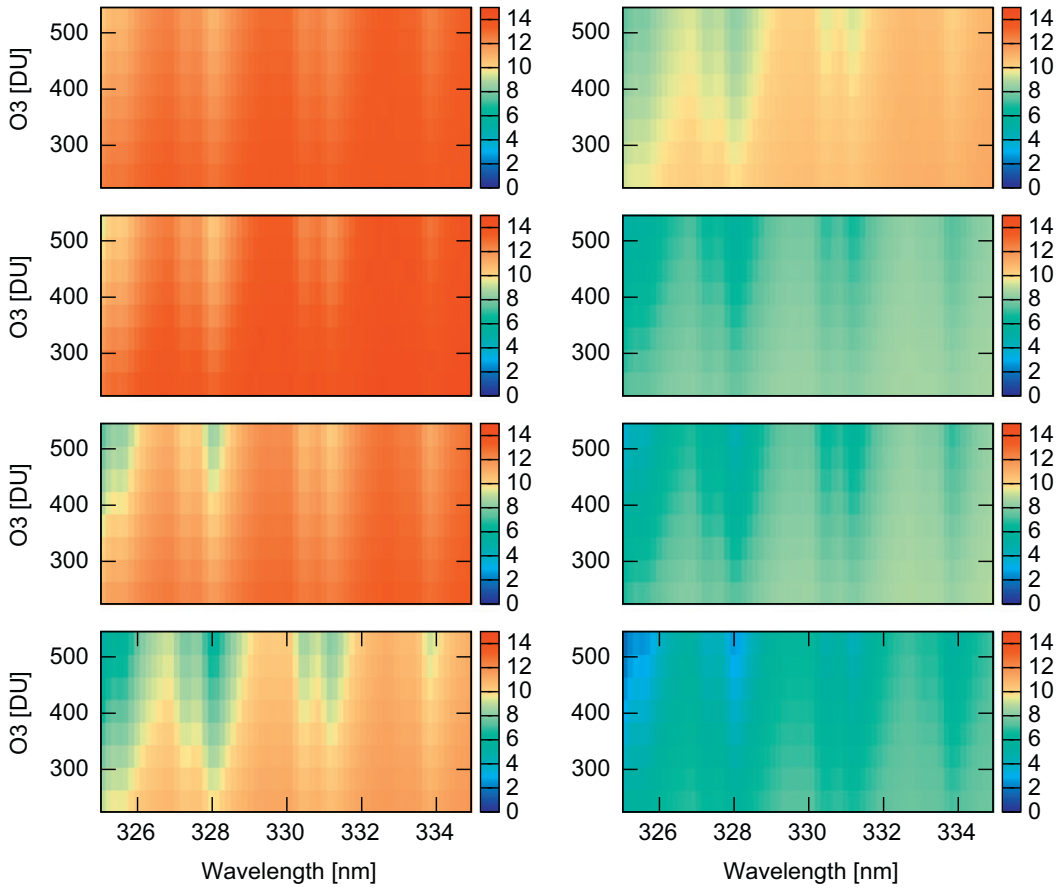

Fig. 5. Contour plots of relative Intensity differences (in %) between SS+2S and SS+L8. Both 2S and L8 calculations are MS only. Scenarios as in Fig. 2.

input/output, and deals with the construction of IOPs that drive the model. The code is in the public domain, and may be obtained free of charge by contacting R.S. at rtsolutions@verizon.net.

At present the code works only for solar sources. It will be implemented as a dedicated module to speed up RT computations for the OCO-2 retrieval algorithm. In the future this will be expanded to also include thermal emission. An important future application will be to develop a PCA methodology in conjunction with the 2S code to speed up radiance calculations across the entire electromagnetic spectrum.

Acknowledgments

This work was performed for the Orbiting Carbon Observatory Project at the Jet Propulsion Laboratory, California Institute of Technology, under a contract with the National Aeronautics and Space Administration.

References

[1] Thomas GE, Stamnes K. Radiative transfer in the atmosphere and ocean. Cambridge University Press; 1999.
[2] Kylling A, Stamnes K, Tsay S-C. A reliable and efficient two-stream algorithm for spherical radiative transfer : documentation of accuracy in realistic layered media. J Atmos Chem 1995;21:115–50.
[3] Toon O, McKay CP, Ackerman TP, Santhanam K. Rapid calculation of radiative heating rates and photodissociation rates in inhomogeneous multiple scattering atmospheres. J Geophys Res 1989;94:16287–301.
[4] Gabriel P, Stephens GL, Wittmeyer IL. Adjoint perturbation and selection rule methods for solar broadband two-stream fluxes in multi-layer media. J Quant Spectrosc Radiat Transfer 2000;65:693–728.
[5] Wiscombe W, Joseph J. The range of validity of the Eddington approximation. Icarus 1977;32:362–77.
[6] Stamnes K, Tsay S-C, Wiscombe W, Jayaweera K. Numerically stable algorithm for discrete ordinate method radiative transfer in multiple scattering and emitting layered media. Appl Opt 1988;27:2502–9.
[7] Crisp D, Atlas RM, Breon F-M, Brown LR, Burrows JP, Ciais P, et al. The orbiting carbon observatory (OCO) mission. Adv Space Res 2004;34:700–9.
[8] Natraj V, Jiang X, Shia R-L, Huang X, Margolis JS, Yung YL. Application of principal component analysis to high spectral resolution radiative transfer: a case study of the O_2 A band. J Quant Spectrosc Radiat Transfer 2005;95(4):539–56, doi:10.1016/j.jqsrt.2004.12.024.
[9] Natraj V, Shia R-L, Yung YL. On the use of principal component analysis to speed up radiative transfer calculations. J Quant Spectrosc Radiat Transfer 2010;111:810–6, doi:10.1016/j.jqsrt.2009.11.004.
[10] O'Dell CW. Acceleration of multiple-scattering hyperspectral radiative transfer calculations via low-stream interpolation. J Geophys Res 2010;115:D10206, doi:10.1029/2009JD012803.
[11] Duan M, Lin Q, Li J. A fast radiative transfer model for simulating high-resolution absorption bands. J Geophys Res 2005;110:D15201, doi:10.1029/2004JD005590.
[12] Rozanov VV, Kurosu TP, Burrows JP. Retrieval of atmospheric constituents in the UV/visible: a new quasi-analytical approach for the calculation of weighting functions. J Quant Spectrosc Radiat Transfer 1998;60:277–99.
[13] Spurr RJD, Kurosu TP, Chance KV. A linearized discrete ordinate radiative transfer model for atmospheric remote sensing retrieval. J Quant Spectrosc Radiat Transfer 2001;68:689–735.
[14] Landgraf J, Hasekamp O, Trautmann T, Box M. A linearized radiative transfer model for ozone profile retrieval using the analytical forward-adjoint perturbation theory. J Geophys Res 2001;106:27291–306.
[15] Liu X, Chance K, Sioris CE, Spurr RJD, Kurosu TP, Martin RV, et al. Ozone profile and tropospheric ozone retrievals from the global ozone monitoring experiment: algorithm description and validation. J Geophys Res 2005;110:D20307, doi:10.1029/2005JD006240.
[16] Spurr R. LIDORT and VLIDORT: linearized pseudo-spherical scalar and vector discrete ordinate radiative transfer models for use in remote sensing retrieval problems. In: Kokhanovsky A, editor. Light scattering reviews, vol. 3. Springer; 2008.
[17] Spurr R. Simultaneous radiative transfer derivation of intensities and weighting functions in a general pseudo-spherical treatment. J Quant Spectrosc Radiat Transfer 2002;75(4):129–75, doi:10.1016/S0022-4073(01)00245-X.
[18] Munro R, Eisinger M, Anderson C, Callies J, Corpaccioli E, Lang R, et al. GOME-2 on METOP: from in-orbit verification to routine operations. In: Proceedings of the EUMETSAT Meteorological Satellite Conference, Helsinki, Finland; 12–16 June 2006.
[19] Levelt PF, van den Oord GHJ, Dobber MR, Mälkki A, de Vries J, Stammes P, et al. The ozone monitoring instrument. IEEE Trans Geosci Remote Sensing 2006;44:1093–101.
[20] Van Roozendael M, Loyola D, Spurr R, Balis D, Lambert J-C, Livschitz Y, et al. Ten years of GOME/ERS-2 total ozone data: the new GOME data processor (GDP) Version 4: I. Algorithm description. J Geophys Res 2006;111:D14311, doi:10.1029/2005JD006375.
[21] Lerot C, van Roozendael M, van Gent J, Loyola D, Spurr R. The GODFIT algorithm: a direct fitting approach to improve the accuracy of total ozone measurements from GOME. Int J Remote Sensing 2010;31:543–50.
[22] Bhartia P. Algorithm theoretical baseline document. TOMS v8 Total ozone algorithm ; 2003. 〈http://toms.gsfc.nasa.gov/version8/version8_update.html〉.
[23] Bodhaine B, Wood N, Dutton E, Slusser J. On Rayleigh optical depth calculations. J Atmos Ocean Tech 1999;16:1854–61.
[24] Malicet J, Daumont D, Charbonnier J, Parisse C, Chakir A, Brion J. Ozone UV spectroscopy. II. absorption cross-sections and temperature dependence. J Atmos Chem 1995;21:263–73.